Decay of passive scalars under the action of single scale smooth velocity fields in bounded two-dimensional domains: From non-self-similar probability distribution functions to self-similar eigenmodes

Jai Sukhatme and Raymond T. Pierrehumbert
Department of Geophysical Sciences, University of Chicago, Chicago, Illinois 60637
(Received 20 June 2002; published 6 November 2002)

We examine the decay of passive scalars with small, but nonzero, diffusivity in bounded two-dimensional (2D) domains. The velocity fields responsible for advection are smooth (i.e., they have bounded gradients) and of a single large scale. Moreover, the scale of the velocity field is taken to be similar to the size of the entire domain. The importance of the initial scale of variation of the scalar field with respect to that of the velocity field is strongly emphasized. If these scales are comparable and the velocity field is time periodic, we see the formation of a periodic scalar eigenmode. The eigenmode is numerically realized by means of a deterministic 2D map on a lattice. Analytical justification for the eigenmode is available from theorems in the dynamo literature. Weakening the notion of an eigenmode to mean statistical stationarity, we provide numerical evidence that the eigenmode solution also holds for aperiodic flows (represented by random maps). Turning to the evolution of an initially small scale scalar field, we demonstrate the transition from an evolving (i.e., non-self-similar) probability distribution function (pdf) to a stationary (self-similar) pdf as the scale of variation of the scalar field progresses from being small to being comparable to that of the velocity field (and of the domain). Furthermore, the non-self-similar regime itself consists of two stages. Both stages are examined and the coupling between diffusion and the distribution of the finite time Lyapunov exponents is shown to be responsible for the pdf evolution.

DOI: 10.1103/PhysRevE.66.056302 PACS number(s): 47.52.+j

I. INTRODUCTION

Starting with the work of Batchelor [1], the study of passive scalars in smooth velocity fields has been the subject of numerous investigations. Originally posed in three dimensions (3D) [1], the problem considered a situation where the viscosity (ν) of the flow is much greater than the diffusivity (κ) of the scalar. Therefore, even at large Reynolds numbers, for length scales below the viscous cutoff (l_ν) and above the diffusive cutoff (l_κ), the so-called Batchelor regime, one has a smooth velocity advecting a diffusive tracer. Since then the problem has grown to encompass a variety of phenomena such as chaotic advection (see, for example, Ottino [2]) and scalars in inverse cascading 2D turbulent flows (see Sec. III in Falkovich *et al.* [3] for a recent review). Of particular interest to us are applications in the realm of geophysical fluid dynamics, specifically, the mixing of scalars along isentropic surfaces via large scale atmospheric flows [4,5].

The equation governing the passive scalar (ϕ) is,

$$\frac{\partial \phi}{\partial t} + (\vec{u} \cdot \vec{\nabla}) \phi = \kappa \nabla^2 \phi. \tag{1}$$

Let us denote the size of the domain by L. This is a linear equation for ϕ, the velocity field is part of the prescribed data. The usual conditions imposed on the velocity field are that it be divergence-free and smooth, i.e., $\vec{\nabla} \cdot \vec{u} = \vec{0}$ and $|\vec{\nabla} \vec{u}| < \infty$ everywhere in the domain. The questions asked are usually of the form: given an initial scalar field is it possible to determine the long time behavior of the solution? Does one see the emergence of an eigenmode with a well-defined decay rate, in other words what is the nature of the spectrum of the advection diffusion operator in a suitably defined function space? Usually, given the aperiodic nature of the advecting velocity fields the question is better posed in a statistical sense, i.e., is the asymptotic probability distribution function (pdf) of the scalar field self-similar or is it an ever evolving (non-self-similar) entity? As things stand, the results found in the literature are fairly divided. One of the aims of this paper is to unify these results by bringing out certain salient features (such as scale separation) that have not been emphasized previously.

Most theoretical studies have focused on the case when the initial scale of variation of the scalar field (say l_s, $l_s \gg l_\kappa$) is much smaller than that of the velocity field (say l_v, we take $l_v \sim L$). The problem then is to determine the statistical properties of the scalar field at scales between l_v and l_κ. A successful approach in this direction has been to shift to a comoving reference frame, use the decomposition $u_\alpha = (\partial_\alpha u_\beta)(t)\, r_\beta = \sigma_{\alpha\beta}(t)\, r_\beta$, and deal with the the effective equation that results from a substitution in Eq. (1) (see, for example, Refs. [6,7] and the references therein). The expectation [7] is that the scalar field will have non-self-similar pdf's. Or, defining the moments of the scalar field as $\langle |\phi(x,y,t)|^n \rangle$, Balkovsky and Fouxon [7] explicitly show that

$$\langle |\phi(x,y,t)|^n \rangle \sim e^{-\alpha_n t}; \quad t > T \tag{2}$$

and that α_n is a nonlinear function of n (T is a diffusive time scale which will be clarified later), implying the non-self-similarity of the pdf's. Recent experiments [8] with passive scalars injected at point sources in inverse cascading 2D turbulent flows seem to validate some of these predictions. Concrete evidence is available from numerical work demon-

strating the nonlinearity of α_n for scalars advected by realistic atmospheric winds [5]. It should be noted that these simulations are over a time scale which represent the transient scalar behavior rather than the asymptotic large time solution.

On the other hand, there is a small body of work that deals with the case when $l_\kappa \ll l_s \sim l_v \sim L$, i.e., the initial scale of variation of the scalar field is comparable to that of the velocity field, both of which are in turn comparable to the scale of the domain.[1] The observation, based on numerical work [10,11], is that the scalar field enters an eigenmode (termed a ''strange eigenmode'' by Pierrehumbert [10] due to its spatial complexity). The pdf of the scalar becomes self-similar (after a suitable normalization by the variance) or in terms of the moments, $\alpha_n \sim n$. Recently, experimental evidence for the emergence of such an eigenmode has been provided in the case of time periodic velocity fields [13]. A line of attack on this problem has been to try and relate the finite time Lyapunov exponents (FTLE's) of the advecting flow to the statistical properties of the scalar field (see Ref. [12] and the references therein). Even though this work [12] is successful in describing the initial stages of the problem, the FTLE's are by definition local entities and appear to be unsuitable precisely when $l_s \sim l_v$.[2]

In this study we work with simple prescribed velocity fields in 2D that have a single large scale (of the kind encountered in studies of chaotic advection). It is worth emphasizing that the power spectrum of such velocity fields is discrete. This is in contrast to technically smooth velocity fields that possess a heirarchy of scales. In other words the velocity fields considered are Lipschitz continuous over all scales of interest (i.e., between l_κ and $l_v \sim L$). The large single scale, divergence-free and smooth nature of the velocity field implies that the trajectory equations do not show explosive (implosive) separation (collapse) as is generally expected in turbulent (or multiple scale) incompressible (compressible) velocity fields (see e.g., Gawedzki and Vergassola [15]).

Our first aim is to give further justification for the eigenmode in periodic and aperiodic velocity fields. We explicitly construct an area preserving deterministic 2D map which, in spite of having weak barriers, demonstrates the emergence of a periodic eigenmode. Moreover, we point out theorems in the dynamo literature, which are applicable to the passive scalar problem, thereby providing analytical justification (in terms of the purely discrete spectrum of the advection diffusion operator) for the eigenmodes. The aperiodic case is free of barriers due to the random nature of the maps employed but is slightly novel in the sense that the notion of an eigenmode has to be weakened by invoking statistical stationarity (i.e., self-similarity of the pdf). Second, we present a unified picture of the two seemingly disparate cases mentioned above. Starting with a scalar field that satisfies $l_s \ll l_v \sim L$, we observe an evolution in the shape of the pdf (i.e., the pdf is non-self-similar). This evolution ceases when the scales of the velocity and scalar fields become comparable (i.e., the field enters an eigenmode with a self-similar pdf). The various regimes that the scalar field encounters are analyzed and a simple example, motivated by the work of Balkovsky and Fouxon [7], is used to elucidate the coupling between diffusion and the distribution of FTLE's and its role in determining the pdf evolution. A discussion of the regimes, their universality, and the issue of scale separation conclude the paper.

II. THE EIGENMODE

A. The eigenvalue problem

Physically when $l_s \sim l_v \sim L$ the scalar field feels the effect of the finite size of the domain, moreover, as $l_s \sim l_v$ it is difficult to justify any linearization of the underlying nonlinear trajectory equations. Fortunately, the linear nature of Eq. (1) lends itself to an eigenvalue analysis. Recently Fereday *et al.* [16] have looked at the eigenvalue problem for a specific velocity field (represented by the Bakers map). We consider the eigenvalue problem in its full generality as has been done for the magnetic field in the kinematic dynamo literature [17–19]. Most of the material in this section is well known in the dynamo literature, we present it here merely to put things in a well-defined framework. Let us recast Eq. (1) as

$$\frac{\partial \phi}{\partial t} = \mathcal{L}_\kappa \phi, \quad \mathcal{L}_\kappa \phi = \kappa \nabla^2 \phi - (\vec{u} \cdot \vec{\nabla}) \phi. \tag{3}$$

For a steady velocity field one can separate time by assuming a solution of the form $\phi(x,y,t) = \overline{\phi}(x,y) e^{\sigma t}$. Hence the eigenvalue problem is

$$\mathcal{L}_\kappa \overline{\phi} = \sigma \overline{\phi}. \tag{4}$$

Here $\overline{\phi} \in B(\mathsf{D})$, where $B(\mathsf{D})$ is a Banach space of square integrable functions[3] defined on the domain D. We take D to be $[0,2\pi] \times [0,2\pi]$ with opposite sides identified (i.e., a torus). The object of interest is the spectrum of the operator $\mathcal{L}_\kappa$ acting in $B(\mathsf{D})$. As we are working in a Banach space of infinite dimensions the spectrum depends strongly on the nature of the operator [20].

[1] We always take $l_v \sim L$. There are other problems of interest where $l_v \ll L$, which are studied in the context of turbulent diffusion (see e.g., the comprehensive review by Majda and Kramer [9]).

[2] A recent paper [14] analyzes the work of Antonsen *et al.* [12] with an aim to understand the exponential decay of scalar moments. This paper, Wonhas and Vassilicos [14], identifies a ''global'' mechanism responsible for the exponential decay and also hints at the importance of the scale separation we have emphasized in this paper.

[3] For *finite* times, given that $|\vec{\nabla} \vec{u}| < \infty$, we are guaranteed that the scalar field will remain square integrable.

If the operator in question were compact,[4] then the spectral theory of finite dimensional operators would carry over to our infinite-dimensional problem [20]. Unfortunately differential operators are usually not compact, moreover they are unbounded. One of the techniques used to handle such operators is to gain control over their resolvents (see Kato [20], Chap. 3), the case when the operator is closed and its resolvent is compact is particularly clear-cut [20]. As it turns out, this is precisely what happens to $\mathcal{L}_\kappa$ for steady velocity fields and nonzero κ, i.e., it is (weakly) closed on $B(\mathsf{D})$ and has a compact resolvent [21].[5] Hence its spectrum consists of a discrete set of eigenvalues of finite multiplicity (Kato [20], p. 187), in fact it has a complete set of eigenfunctions [21]. Physically the implication of a purely discrete spectrum is that the eigenvalues are well separated, as time goes on $\overline{\phi}(x,y)$ will assume the form of the eigenfunction corresponding to the largest eigenvalue. In the more general case of a periodic velocity field we have to consider the Floquet problem involving the propagation of $\phi(x,y,t)$ to $\phi(x,y,t+T)$ where T is the periodicity of the underlying flow. Denoting the propagator by $\mathcal{T}_\kappa(T)$, the eigenvalue problem is of the form

$$\mathcal{T}_\kappa(T)\,\overline{\phi}=e^{pT}\ \ \overline{\phi}. \tag{5}$$

The discreteness of the spectrum of $\mathcal{T}_\kappa$ persists but the existence of a complete set of eigenfunctions is not gauranteed [21]. Essentially when the flow is smooth and $\kappa>0$, we are assuming that the spectral properties of $\mathcal{L}_\kappa$ follow those of $\mathcal{M}_\kappa$ [Eq. (6)] for which there exist rigorous results in the cited dynamo literature. So, from a mathematical point of view, the problem has a purely discrete set of eigenvalues and a (possibly incomplete) set of eigenfunctions for both steady and time periodic velocity fields. In passing, we mention that the $\kappa\to 0$ limit is expected to be quite delicate; interesting aspects not encountered in the $\kappa\neq 0$ problem are likely to appear in this limiting process (see Bayly [18] for some illuminating examples in regard to the analogous scalar dynamo problem).

[4]Consider an infinite sequence of functions $\psi_1,\psi_2,\ldots$ in a complete function space. Let us denote the action of an operator A on these functions by the sequence $A\psi_1,A\psi_2,\ldots$. If A is closed with respect to this space and further if one can extract a convergent subsequence from $A\psi_1,A\psi_2,\ldots$ then A is called a compact operator.

[5]The cited Ref. [21] deals with a similar operator that appears in the magnetic dynamo theory, specifically the operator they work with is

$$\mathcal{M}_\kappa\vec{B}=\kappa\nabla^2\vec{B}-(\vec{u}\cdot\vec{\nabla})\vec{B}+\vec{B}\cdot\nabla\vec{u}, \tag{6}$$

where $\vec{B}$ is the magnetic field. The difference in $\mathcal{L}_\kappa$ and $\mathcal{M}_\kappa$ is the additional ''stretching'' term in $\mathcal{M}_\kappa$. As this term does not contain derivatives of $\vec{B}$, it is quite intuitive that the spectral properties of $\mathcal{M}_\kappa$ should carry over to $\mathcal{L}_\kappa$. In fact, it is quite reasonable that as long as the gradients of the velocity field are bounded, the spectral properties of both $\mathcal{L}_\kappa$ and $\mathcal{M}_\kappa$ follow those of the Laplacian as the highest-order derivatives are contained in the Laplacian term.

B. Deterministic maps (periodic velocity fields)

We proceed to see if we can numerically realize the eigenfunctions corresponding to the above-mentioned eigenvalues. Chaotic maps on a lattice are utilized to represent the advection process (see Pierrehumbert [11] for a succinct overview of lattice maps in advection). The advantage of the lattice maps is the exact preservation of scalar moments and their numerical efficiency. This ''pulsed'' advection is followed by a diffusive step (e.g., see Ref. [11] or [10]). Usually maps with random phase shifts at each iteration are employed so as to break the Kolmogorov-Arnold-Moser (KAM) tori that are generically present in deterministic area preserving maps. As this procedure gives an aperiodic time dependence to the flow, it is unacceptable in the eigenvalue formulation outlined in the preceding section. Unfortunately, we are unaware of any area preserving, nonlinear, and continuous map that has been proven to be mixing[6] over the whole domain D. The only way we have of seeing that there are no regions where the scalar field remains trapped is to do so numerically, i.e., to examine the variance as a function of time. The particular map we use mimics an alternating nonlinear shear flow,

$$\begin{aligned} x_{n+1}&=x_n+A_1\,\sin(B_1y_n+s_1)+A_2\,\sin(B_2y_n+s_1)\\ y_{n+1}&=y_n+C_1\,\sin(D_1x_{n+1}+s_2)+C_2\,\sin(D_2x_{n+1}+s_2). \end{aligned} \tag{7}$$

Here s_1,s_2 are constant random numbers used to get the sine functions out of phase and x_n,y_n are mod$(0,2\pi)$. The constants are $A_1=4,B_1=1,A_2=1,B_2=\pi,C_1=1,D_1=1,C_2=\frac{1}{4},D_2=\pi/2$ and the initial condition of the scalar field is $\phi(x,y)=\cos(x)\cos(y)$ (note that the scale of the scalar field is comparable to the scale of the flow). The diffusive step is implemented as

$$\phi_{i,j}=(1-D)\,\phi_{i,j}+\Delta\phi_{i,j}, \tag{8}$$

where $\Delta\phi_{i,j}$ is

$$\Delta\phi_{i,j}=\tfrac{1}{4}D(\phi_{i+1,j}+\phi_{i-1,j}+\phi_{i,j+1}+\phi_{i,j-1}). \tag{9}$$

Here $0<D<1$ is the diffusion coeffecient and i,j are the indices of the lattice. As is expected, for certain combinations of s_1,s_2 there are persistent KAM barriers and we do not observe a decay of the scalar variance as would be expected from a globally mixing system. In fact, after a short time the diffusive exchange across the barriers controls the variance. $s_1=0,s_2=0$ provides an example of this phenomenon, Fig. 1 shows the variance as a function of time for $D=0.5$, 0.4, 0.3, and $D=0.2$, the control of the variance by the diffusion coefficient is evident, moreover, a certain amount of scalar is trapped within the barriers (the trapping would be permanent as $\kappa\to 0$, though the scaling of the amount that diffuses as a function of κ is expected to be nontrivial [23]).

[6]Mixing in the sense of dynamical systems (see e.g., Ref. [22]).

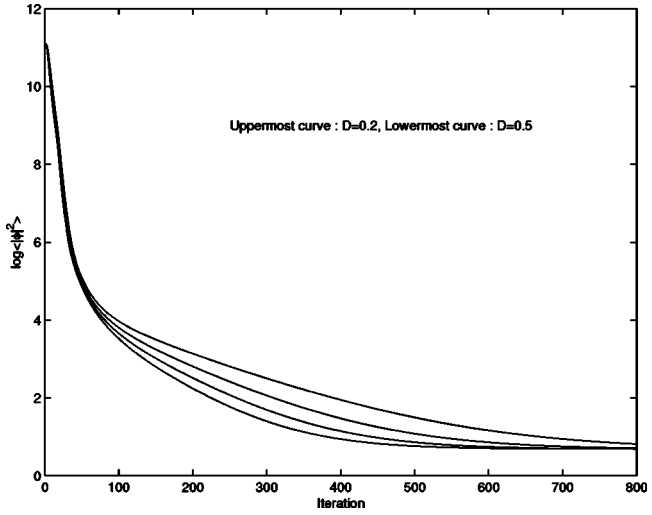

FIG. 1. The strong barrier case: The decay of the natural logarithm of the variance for different diffusivities.

On the other hand, we get the desired global decay (down to machine precision) accompanied by the emergence of a periodic eigenmode for other pairs of s_1, s_2, (namely, $s_1 = 5.9698$, $s_2 = 1.4523$, and $D = 0.5$). Apart from using $\phi(x,y) = \cos(x)\cos(y)$ as an initial condition, we also carried out the simulation using a checkerboard-type initial condition where the field is discontinous but square integrable (the initial conditions can be seen in the upper panel of Fig. 2). The spatial structure of the eigenmode at iteration 250 and 650 for the first initial condition can be seen in the first column of Fig. 2. The second column of Fig. 2 shows the evolution of the scalar field for the second initial condition (the eigenmode is shown at iteration 250 and iteration 650). The upper panel of Fig. 3 shows a log plot of the moments as a function of iteration.[7] The perfectly normal scaling, i.e., $\alpha_n \sim n$, [refer Eq. (2)] is shown in the middle panel of Fig. 3. Finally the self-similar pdf's in steps of 25 iterations from iteration 250 to 650 can be seen in the lowermost panel of Fig. 3. Figure 4 shows the same entities for the second initial condition (see figure caption for details). The bimodal nature of the pdf indicates that there still exist regions that remain relatively isolated from each other. In a sense these regions are ''large enough'' to permit chaotic advection of the scalar within themselves and the barriers are ''leaky enough'' so the exchange of the scalar across them is strong enough so as *not* to be a controlling factor. Note that due to the existence of these barriers, the value of D has to be reasonably large (in our experiments the results for α_n were identical for $D > 0.2$), if the system was mixing without any barriers then the results would be valid for infinitesimally small diffusivity.

Though the emphasis in the dynamo literature has been on the infinite magnetic Reynolds number limit, there have been a few studies on the form of the eigenfunctions at finite magnetic Reynolds numbers. The maps used in these studies are chosen for their mathematical properties (such as the Bakers map in Ref. [24] or the Cat map on an unusual Reimannian manifold in Ref. [25]), i.e., one has good mixing properties over the whole domain. Also, these maps allow analytical estimates of the form of the eigenfunctions, hence provide some insight into the generically singular infinite magnetic Reynolds number limit (in terms of convergence to some eigendistribution [19]). Unfortunately such maps are slightly unphysical, their chaotic properties are due to boundary conditions or due to the curvature of the underlying manifold

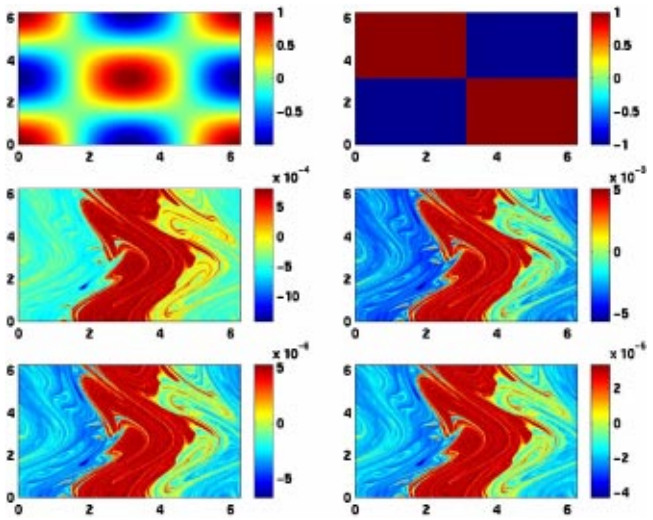

FIG. 2. The weak barrier case. Upper panels: The two initial conditions. Middle panels: The eigenmodes after 250 iterations. Lower panels: The eigenmode after 650 iterations.

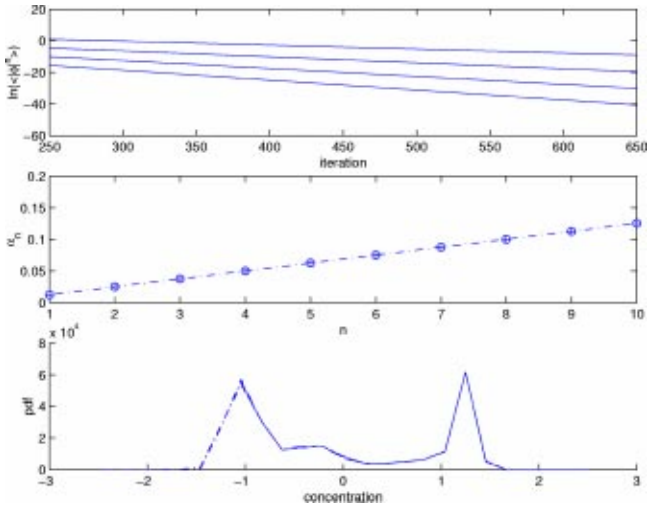

FIG. 3. The weak barrier case. Upper panel: The decay of the various moments ($n = 2, 3, 4$, and 5 with the higher moments appearing lower on the figure) for the first initial condition. Middle panel: The extracted values of α_n vs n (the dash-dot line marked with circles), "+" is a plot of $n\alpha_1$. Lower panel: The pdf's in steps of 25 iterations from iteration 250 to 650 for the first initial condition. The pdf's lie on top of each other due to their self-similar nature.

[7]The higher moments involve a fair degree of numerical uncertainly, even though they do appear to behave as expected, we feel it is better to rely on the pdf's themselves.

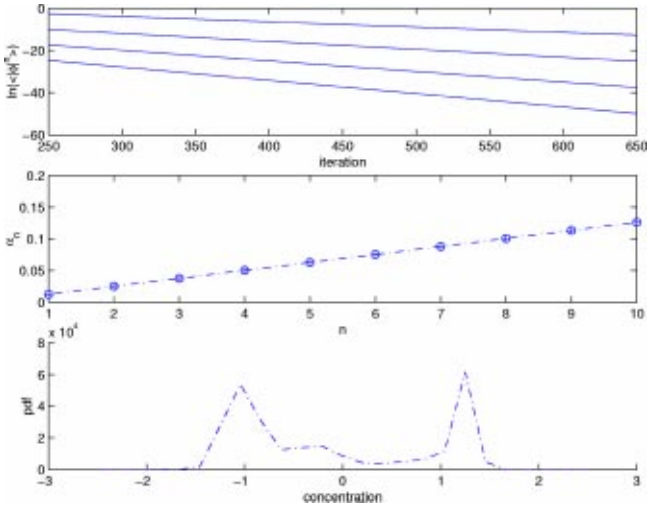

FIG. 4. The weak barrier case. Upper panel: The decay of the various moments ($n=2, 3, 4,$ and 5 with the higher moments appearing lower on the figure) for the second initial condition. Middle panel: The extracted values of α_n vs n (the dash-dot line marked with circles), "+" is a plot of $n\alpha_1$. Lower panel: The pdf's in steps of 25 iterations from iteration 250 to 650 for the second initial condition. Once again, the pdf's lie on top of each other due to their self-similarity.

rather than any inherent nonlinearity in the maps themselves. Even though we choose not to use such maps for advective purposes, we would like to mention that their results (especially Ref. [24]) are consistent with our work.

C. Random maps (aperiodic velocity fields)

In the aperiodic case there is no clean way to separate time from space as was done in the earlier situations. Due to this we weaken the notion of an eigenfunction by invoking statistical stationarity, i.e., the scalar field is said to enter an eigenmode when the shape of its pdf remains invariant with time (upon renormalization by its variance as the overall field strength is decaying). Note that the earlier classical eigenmode also has self-similar pdf's. Of course, it has a stronger form of convergence where the scalar field itself approaches a stationary (or periodic) spatial structure. The random map used to represent the aperiodic flow is again a nonlinear shear flow,

$$x_{n+1}=x_n+4\sin(y_n+p_n),$$

$$y_{n+1}=y_n+\sin(x_{n+1}+q_n). \tag{10}$$

Now p_n, q_n ($\in[0,2\pi]$) are random numbers selected at the beginning of each iteration. x_n, y_n are mod$(0,2\pi)$, $D=0.25$ and the initial scalar field is $\phi(x,y)=\cos(0.5x)\cos(0.5y)$. The map is iterated till the variance goes down to machine precision. The variance as a function of time can be seen in the upper panel of Fig. 5. After an initial transient (which lasts for about 10 iterations, see Ref. [12]) the variance decays exponentially. The higher moments can be seen in the lower panel of Fig. 5. The nonanomalous nature of the exponents can be seen in the upper panel of Fig. 6, the implied

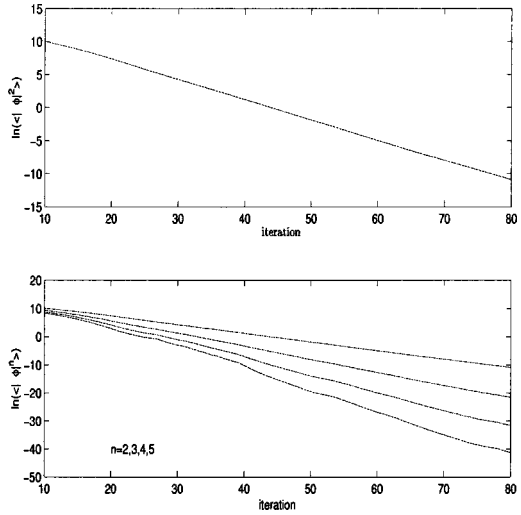

FIG. 5. The aperiodic (no barrier) case. Upper panel: The decay of the variance. Lower panel: The higher-order moments (progressively higher moments appear lower on the figure).

self-similar behavior of the pdf of the scalar field is demonstrated in the lower panel of Fig. 6. The pdf is unimodal as there are no isolated regions in the domain (the randomness at each iteration is responsible for the destruction of any barriers that might exist in the steady map). Moreover, the shape of the pdf is characterized by a Gaussian core and stretched exponential tails, as per the higher resolution studies by Pierrehumbert [11].

D. Physical interpretation

The physical picture that goes along with the eigenmode is as follows: Consider a filament of scalar whose length is comparable to the scale of variation of the velocity field (or the typical size of an eddy in the velocity field). Due to the assumed chaotic properties of a generic time dependent 2D flow, the filament will tend to be stretched out. The point is that, as the scale of the filament is already the same as that of the flow, instead of being merely stretched the filament will

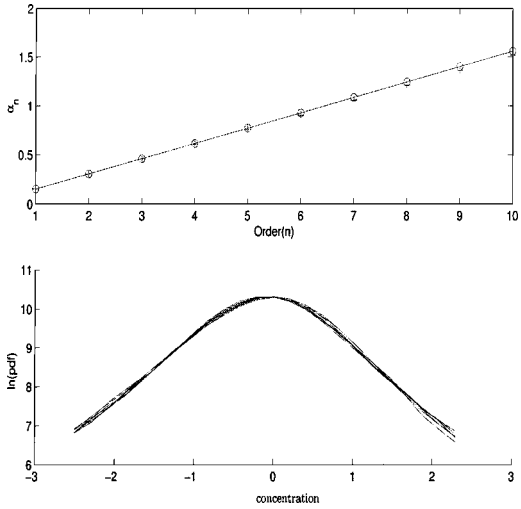

FIG. 6. The aperiodic (i.e., no barrier) case. Upper panel: α_n vs n(o), the dash-dot line is $n\alpha_1$. Lower panel: The self-similar pdf's.

fold and start to fill the eddy. This process continues till the filament has been ''packed'' as tightly possible. Note that it is the diffusion that is responsible for the ''packing,'' i.e., for $\kappa>0$ there is a limit on how thin a filament can get. Once this situation is reached, as the problem is unforced, the whole structure remains stationary (or periodic or statistically stationary depending on the flow) till the diffusion destroys all the variance in the scalar field. We argue that the eigenmode is a representation of this ''packed'' structure.

III. THE DIFFERENT REGIMES

Having got a feel of the situation when the initial scale of variation of the scalar field and that of the velocity field are comparable, we proceed to look into the evolution of an initially small scale scalar field, i.e., $l_\kappa \ll l_s \ll l_v \sim L$.

As $\phi \in B(D)$, via Fourier's theorem, we can represent ϕ as

$$\phi(\vec{r},t)=\int_{\vec{k}_0} \hat{\phi}(\vec{k}_0,t)e^{i\vec{k}(t)\cdot\vec{r}}d\vec{k}_0. \tag{11}$$

Substituting a plane wave solution in Eq. (1) and equating the real and imaginary parts, we get,

$$\frac{\partial\hat{\phi}(\vec{k}_0,t)}{\partial t}=-\kappa|\vec{k}(t)|^2\hat{\phi}(\vec{k}_0,t), \tag{12}$$

where $\vec{k}(t)$ is given by

$$\vec{r}\cdot\frac{\partial\vec{k}(t)}{\partial t}=-\vec{u}\cdot\vec{k}(t); \quad \vec{k}(0)=\vec{k}_0. \tag{13}$$

A. Small time scales

In the eigenvalue formulation, when $l_s \ll L \sim l_v$ the scalar field is essentially in an infinite domain, the implication is that the spectrum of $\mathcal{L}_\kappa$ now typically consists of a continuous part and hence possesses eigenvalues that lie arbitrarily close to each other. As there is no dominant eigenvalue, we will not see the emergence (at short times) of the corresponding eigenmode.

Taking advantage of $l_s \ll l_v$, we linearize Eq. (13) to obtain

$$\frac{\partial\vec{k}(t)}{\partial t}=-\vec{\nabla}\vec{u}(\vec{k}_0,t)\vec{k}(t). \tag{14}$$

From Eq. (12) we have

$$\hat{\phi}(\vec{k}_0,t)=\hat{\phi}(\vec{k}_0,0)e^{-\kappa\int_0^t|\vec{k}(s)|^2ds}. \tag{15}$$

Therefore, in order to see how the moments behave at small times we need an estimate of how $|\vec{k}(t)|$ evolves. Generally this is a fairly intricate question as the solution to Eq. (14) involves a time ordered exponentiation that reduces to a product of matrices [26].

1. Useful properties of the FTLE's

We mention some of the properties of the FTLE's that will be needed for calculations in the forthcoming sections. In 2D we have the possibility of 2 (asymptotic) Lyapunov exponents. Let us denote the larger of these by Λ_0. Furthermore let us denote the FTLE along a particular trajectory, after n iterations, by $\Lambda(n)$. Note that physically the FTLE's are defined with respect to the change in volume of a given set of initial conditions. In 2D incompressible systems, this only depends on the larger eigenvalue in the abovementioned matrix product. In higher dimensions the situation is more complicated as the FTLE depends on the sum of the positive eigenvalues (for continuous flows) of the matrix product, i.e., it is closely related to the topological entropy of the dynamical system.

In D dimensions one has the possibility of D (asymptotic) Lyapunov exponents. Let us denote them by $\Lambda_i (i=1:D)$. It is generally assumed that, along a particular trajectory, the probability of $\Lambda_i(n)$ (i.e., the spectrum of Lyapunov exponents calculated after n iterations) deviating from Λ_i decays exponentially with n [27]. In fact it is generally taken for granted that each $\Lambda_i(n)$ is governed by the central limit theorem (CLT) and is distributed around Λ_i [28] (see also the discussion in Sec. 9.4 of Ref. [29]). We would like to mention that we are not aware of a general proof of this statement. Having said this, we mention that the results of Balkovsky and Fouxon [7] appear to lead in this direction though the status of the proof of the general statement is not very clear. The specific results we are aware of start with the work of Furstenberg (see Ref. [26]), who showed that if the matrices are i.i.d (i.e., δ-function correlated in time) random matrices and if the system is incompressible, then Λ_0 $[=\max(\Lambda_i)]>0$. A stronger result, which is valid only in 2D, has recently been shown by Chertkov *et al.* [6]. It states that if the tangent maps are random matrices with arbitrary (but finite) correlation time then $\Lambda_0>0$, moreover $\Lambda(n)$ obeys the CLT and is distributed around Λ_0.

Therefore, using the CLT for $\Lambda(n)$ in 2D, the distribution of the FTLE's can be expressed as (see Sec. 8.6.4 of Ref. [30] for the large deviation result)

$$Q(\Lambda,n)\sim e^{-nG(\Lambda-\Lambda_0)}, \tag{16}$$

where $G(\Lambda-\Lambda_0)$ is the Cramer function and Λ_0 is the asymptotic Lyapunov exponent. Due to the mixing nature of the system, as $n\to\infty$ the FTLE's along (almost) every trajectory will tend to Λ_0, moreover, the average of many realizations along a particular trajectory can be interpreted as a spatial average [22].

2. The scalar pdf

At this initial stage the problem is completely reversible in the sense that the area of a given blob of scalar is invariant. Physically when we release a small blob of scalar in a chaotic flow, the tendency is for the blob to form a filament while respecting the conservation of area. Mathematically, this implies that on average $\vec{k}(t)$ grows with time, i.e., one of the components of $\vec{k}(t)$ increases while the other one de-

creases. The inference from Eq. (15) is that the moments of the scalar field decay in faster than exponential fashion (see e.g., Refs. [31,32]).

Keeping in mind that the backwards in time problem has the same FTLE's as the forward problem, we can envision a blob of scalar at a time t to have resulted from the diffusive homogenization of a filament (at $t=0$) that has undergone advective collapse [11]. As the initial scale of variation of the scalar field is very small, in effect the blob is a result of the diffusive homogenization of a large number of independent random concentrations. Denoting the scale of the blob by l, for one realization, the probability of the blob's concentration being $\phi=\phi_1$ at time t is [11]

$$P(\phi_1)_t \sim e^{-[le^{\Lambda t}/l_s]S(\phi_1)}, \tag{17}$$

where $S(\phi)$ is the Cramer function. For notational simplicity, we have taken the mean of the random concentrations making up the blob to be zero. Note that the chaotic nature of the flow is embedded in the exponential prefactor to $S(\phi)$. For many realizations the average probability of the above event is

$$\langle P(\phi_1)_t \rangle \sim \int e^{-[le^{\Lambda t}/l_s]S(\phi_1)-tG(\Lambda-\Lambda_0)} d\Lambda. \tag{18}$$

Here $\langle \cdot \rangle$ represents an average of many realizations along a particular trajectory. As mentioned, this can be interpreted as a spatial average. By a steepest descent argument the value of Λ that dominates the above integral satisfies (denoting it by Λ_1)

$$-\frac{l}{l_s} S(\phi_1) e^{\Lambda_1 t} = G'(\Lambda_1-\Lambda_0). \tag{19}$$

As $S(\phi)\geqslant 0$, Eq. (19) implies $\Lambda_1 \leqslant \Lambda_0$. Substituting in Eq. (18), we have

$$\langle P(\phi_1)_t \rangle \sim e^{G'(\Lambda_1-\Lambda_0)} e^{-\beta t}; \quad \beta = G(\Lambda_1-\Lambda_0). \tag{20}$$

Therefore the probability of a particular deviation decays exponentially with a rate β. The important point is that β is a function of the deviation through Λ_1. As $S(\phi)$ is convex [30], for $\phi=\phi_2$ (where $|\phi_2|>|\phi_1|$), $S(\phi_2)>S(\phi_1)$. From Eq. (19) the dominant FTLE for ϕ_2 (denoting it by Λ_2) satisfies $\Lambda_2<\Lambda_1$. Therefore the probability of a large deviation is governed by the smaller FTLE's, i.e., the tails of the pdf of ϕ are sensitive to the tails of the FTLE distribution. At the other extreme, as $\phi \to 0$ we have $\Lambda_1 \to \Lambda_0$ [because $S(\phi)\to 0$ as $\phi \to 0$ and $G'(\Lambda-\Lambda_0)\to 0$ as $\Lambda \to \Lambda_0$]. Also, $S(\phi) \sim \phi^2$ for small deviations. From Eq. (17) the implication is that, in this regime, the scalar pdf has a Gaussian core with a width that decreases in time.

3. Numerical results

To numerically verify these predictions we use the map

$$x_{n+1} = x_n + A \sin(By_n + \psi_n) \mod(0,12\pi),$$

$$y_{n+1} = y_n + C \sin(D_1 x_{n+1} + \sigma_n) \mod(0,12\pi), \tag{21}$$

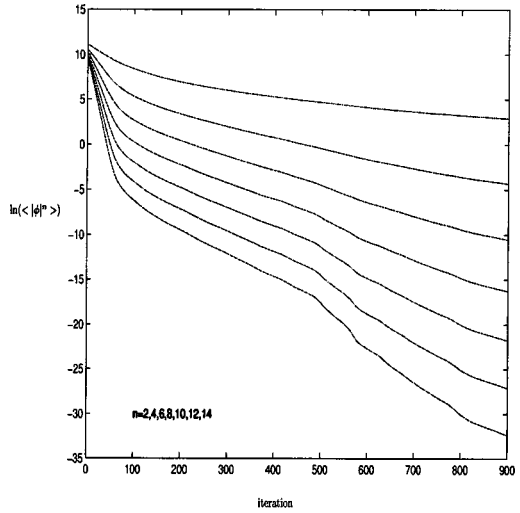

FIG. 7. The decay of the moments for a scalar field whose initial scale of variation is small as compared to that of the advecting flow (the higher moments are lower on the figure).

where ψ_n, σ_n ($\in[0,2\pi]$) are random numbers chosen at the beginning of each iteration, $B=D_1=\frac{1}{6}$ so as to make the scale of the flow comparable to the scale of the domain and $A=1, C=1$. Diffusion is represented as in Eq. (8) with $D=0.25$. To satisfy $l_s \ll l_v$, we take the initial scalar field to be $\phi(x,y)=\cos(4x)\cos(4y)$. Figure 7 shows the evolution of the moments for an ensemble average over 25 realizations of the map. The faster than exponential decay of the moments is visible for the first 90–100 iterations. Moreover, the pdf evolution (in steps of 10 iterations) seen in Fig. 8 goes along theoretical expectations.

B. Intermediate time scales

In Fig. 7 there is a transition from faster than exponential to purely exponential decay of the moments at around iteration 100. This transition is a diffusive effect (the diffusive time T in the Introduction refers to the time at which this

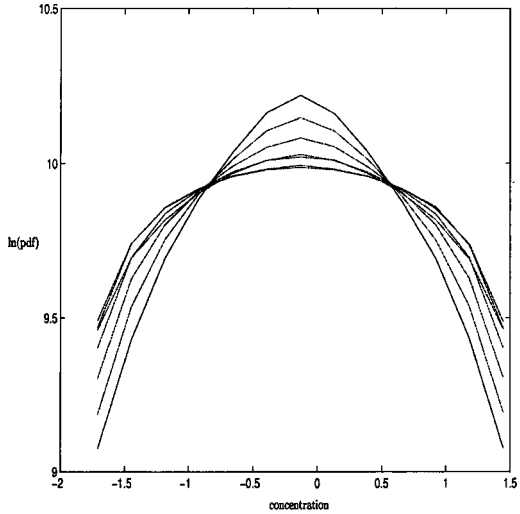

FIG. 8. The pdf's from iteration 40 to 100 (thick line at iteration 100) for the initially small scale scalar field.

transition occurs). As mentioned, from Eq. (15) it is evident that the growing component of $\vec{k}(t)$ controls the decay of $\phi(\vec{k}_0,t)$. In physical space the growing component of $\vec{k}(t)$ represents a shrinking physical scale. As there is a lower limit to this shrinking scale (i.e., l_κ), the magnitude of $\vec{k}(t)$ saturates when its growing component becomes comparable to l_κ^{-1}. From this time onwards $|\vec{k}(t)|^2$ fluctuates around l_κ^{-2} and hence $\phi(\vec{k}_0,t)$ decays in a purely exponential fashion. Physically, even though the flow is incompressible, due to the nonzero diffusivity, the area of a blob of scalar is no longer invariant. In fact, the area increases exponentially, implying an exponential decay of the scalar concentration within the blob itself.

1. Existing results on α_n

In this regime, where both $l_s \ll L \sim l_v$ and the area of a given blob of scalar evolve, the moments of the scalar field have been dealt with in detail by Balkovsky and Fouxon [7]. Their approach involves shifting to a comoving reference frame and using the effective equation [7,6],

$$\frac{\partial \phi}{\partial t} + \sigma_{\alpha\beta} r_\beta \nabla_\alpha \phi = \kappa \nabla^2 \phi. \tag{22}$$

The essential point is that now the trajectory equation takes the form

$$\frac{\partial r_\beta}{\partial t} = \sigma_{\alpha\beta}(t) r_\beta. \tag{23}$$

For this problem the Lyapunov exponents are defined as (see e.g., Ref. [6]),

$$\lambda(t) = \frac{1}{t} \ln \frac{|\vec{r}(t)|}{|\vec{r}(0)|}. \tag{24}$$

Due to the effective space-time separation of the velocity field in the comoving reference frame, $\lambda(t)$ is only a function of time. In effect the behavior of $\Lambda(n)$ for a given trajectory in the FTLE formalism is now valid for the entire domain. In fact, the aforementioned results of Chertkov *et al.* [6] are actually shown in the comoving framework for $\lambda(t)$. Building on this framework, Balkovsky and Fouxon [7] derive expressions for the moments of the scalar field by considering the evolution of an inertia tensorlike quantity for a blob of scalar. The advantage of the inertia tensorlike quantity is that its evolution explicitly captures the exponential growth of a blob's area that characterizes this regime. The chief assumption is that the eigenvalues of the inertia tensor, at any finite time *t*, are governed by the CLT and are distributed about the asymptotic Lyapunov exponents $\lambda_i (i=1,2$ in 2D). With this they are able to show that $\langle |\phi(t)|^n \rangle \sim e^{-\alpha_n t}$ and that α_n is a nonlinear function of *n*, implying a non-self-similar pdf for the scalar field.

2. A simple example of a single non-self-overlapping blob

We present a simple example to put some of the notions regarding the behavior of α_n in perspective. The objective is to analyze the evolution in concentration of a single non-self-overlapping[8] blob. Let the blob's concentration be C_T (at time $t=T$). Now, the increase in the area of the blob is controlled by the FTLE at the position of the blob. Therefore we have

$$C_t = C_T \, e^{-\Lambda(t-T)}; \quad t \geqslant T. \tag{25}$$

Hence,

$$\langle |C_t|^n \rangle = |C_T|^n \int e^{-n\Lambda(t-T)} Q(\Lambda,t) d\Lambda, \tag{26}$$

where $\langle \cdot \rangle$, as before, indicates an average of many realizations over one trajectory. Therefore we have

$$\langle |C_t|^n \rangle = |C_T|^n \int e^{-n\Lambda(t-T) - tG(\Lambda-\Lambda_0)} \, d\Lambda. \tag{27}$$

By a steepest descent argument, for $t \gg T$, the above integral is dominated for $\Lambda = \Lambda^*$ (implicitly) given by

$$\left. \frac{dG}{d\Lambda} \right|_{\Lambda=\Lambda^*} = -n. \tag{28}$$

This implies $\Lambda^* < \Lambda_0$, moreover, for small *n* Eq. (28) implies $\Lambda^* \to \Lambda_0$. In this region the Cramer function is parabolic, i.e., taking $G(\Lambda-\Lambda_0) = a(\Lambda-\Lambda_0)^2$ we have

$$\Lambda^* = \Lambda_0 - \frac{n}{2a}. \tag{29}$$

Substituting back, we obtain (for small *n*)

$$\langle |C_t|^n \rangle \sim e^{-\alpha_n t}; \quad \alpha_n = n\left(\Lambda_0 - \frac{n}{4a} \right). \tag{30}$$

Immediately it is clear that the pdf of the scalar field will be non-self-similar as α_n is a nonlinear function of *n*. Furthermore, the nonlinearity is due to the fact that there is a distribution of FTLE's. If we had a single FTLE or if the FTLE distribution collapsed to a δ function in a short time, then the scaling would be nonanomalous with $\alpha_n = n\Lambda_0$. Note that the explicit expression for α_n given in Eq. (30) is only valid for small *n*. From Eq. (28) the higher moments (as in the previous regime) are sensitive to the smaller FTLE's. As our simple example follows Balkovsky and Fouxon's work, their form for α_n (through more detailed considerations that take into account the diffusive overlap of many blobs) is similar to Eq. (30) (see Eq. (3.9) in Ref. [7]). We reiterate that even though the FTLE distribution is responsible for the pdf evo-

[8]What we mean by ''non-self-overlapping'' is a single blob that stretches and folds in this large scale velocity field but the filaments of the blob do not overlap with each other in these intermediate time scales.

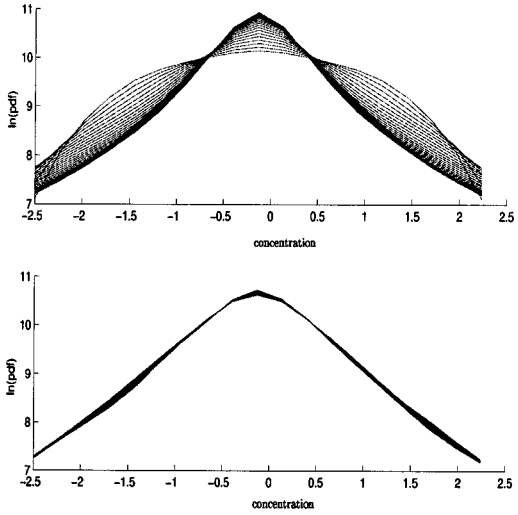

FIG. 9. Initailly small scale scalar field. Upper panel: pdf's from 90–490 (non-self-similar). Lower panel: pdf's from 600–800 (self-similar).

lution in this regime, fundamentally this is still a diffusive effect (in the sense that it is the nonzero diffusivity that leads to the area evolution that characterizes this regime).

3. Numerical results

The upshot of these considerations is that at these intermediate time scales we should observe an evolution in the pdf of the scalar field. To verify this, we plot the pdf's (in steps of 10 iterations from iteration 90 to iteration 490) in the upper panel of Fig. 9. The non-self-similarity is clearly evident. The anomalous nature of α_n can be seen in Fig. 10. We observe that the pdf's are characterized by a (progressively smaller) Gaussian core and (progressively fatter) stretched exponential tails. Interestingly after about iteration 400 the tails of the pdf tend to relax back to a purely exponential form (which is the theoretically expected shape, see Sec. III B in Falkovich *et al.* [3]). The only discrepancy with theoretical predictions [7] is that α_n does not saturate at high n, this might be due to the fact that we are unable to get to high enough n numerically to actually observe the saturation (see the example in the Discussion).

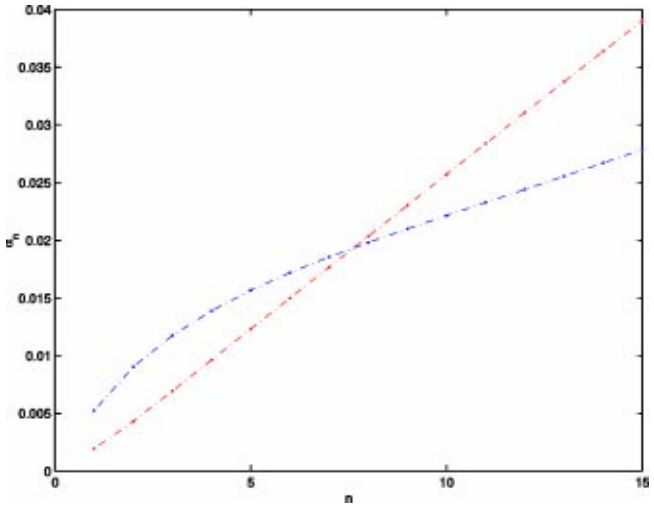

FIG. 10. Initially small scale scalar field: α_n vs n (nonlinear—iteration 90–490, linear—iteration 600–800).

C. Large time scales

From the preceding arguments it would appear that the scalar pdf is an ever-evolving entity (as is implied in [7]), but once again from Fig. 7 we see that the behavior of the moments undergoes another change between iterations 500–600. We claim that it is at this stage that the scalar field actually enters the eigenmode, i.e., beyond iteration 600 the pdf should become self-similar. The lower panel of Fig. 9 shows the pdf's (again in steps of 10 iterations from iteration 600 to iteration 800). The self-similar nature of the pdf's is clearly evident, also α_n (shown in Fig. 10 along with the α_n from the previous regime) follows $\alpha_n \sim n$. Physically the scale of variation of the scalar field is now comparable to that of the velocity field, hence the velocity field separation used to derive Eq. (22) is invalidated. Correspondingly, in the FTLE formulation, the linearization breaks down. In fact, the problem is now in a situation where the mathematical considerations leading to the eigenmode (Sec. II) become applicable.

IV. DISCUSSION

In the first part of the paper we described the behavior of a scalar field whose initial scale of variation was comparable to that of the advecting flow (both of which were similar to the size of the domain). In both periodic and aperiodic situations we demonstrated the emergence of scalar eigenmodes. In spite of the weak barriers that exist in the deterministic map used for periodic flows, the emergence of a scalar eigenmode is robust (as is seen from the two different initial conditions). In the case of random maps, representing aperiodic flows, the mixing is global (as the barriers are destroyed) and the eigenmode is statistical in nature. Along with the recent work of Fereday *et al.* [16], this indicates that passive scalar advection diffusion in chaotic flows can be insightfully treated as an eigenvalue problem as is commonly done for steady flows (see e.g., Young *et al.* Ref. [33]).

We then looked at the evolution of a passive scalar whose initial scale of variation was small as compared to that of the advecting flow (again, the scale of the flow was comparable to the size of the domain). Initially, as has been noted in previous studies [31,32], the moments of the scalar field decay in a faster than exponential fashion. The pdf of the scalar field in this initial regime is an evolving entity, it is shown to be characterized by a Gaussian core that shrinks with time. When the scalar filaments reach the diffusive scale the behavior of the moments experiences a transition to a purely exponential decay. We emphasize that this transition is a diffusive effect. In this intermediate regime the pdf of the scalar field is still an evolving entity (as is shown by Balkovsky and Fouxon [7], via the nonlinear dependence of α_n on n). By means of a simple example, the nonlinear nature of α_n is shown to be dependent on the distribution of FTLE's, more-

over, the higher moments are seen to be sensitive to the tails of the FTLE distribution. Finally, when the scalar filamants have stretched and folded to fill the domain (or have been ''packed'' as per our previous nomenclature) the field enters an eigenmode. The eigenmode, as before, is characterized by self-similar pdf's. Numerical results of advection on a lattice followed by diffusion appear to confirm these stages of evolution.

The above-mentioned stages, which an initially small scale scalar field encounters, are robust, i.e., once one enters a particular stage, the statistical properties of the scalar field are fixed. A caveat is that the duration of the stages strongly depends on the strength of the advecting flow. As an illustration, consider the same scalar field and map as in Eq. (21), but set $A=C=5$ (i.e., a flow with stronger stretching properties). The behavior of the moments and α_n is shown in Fig. 11 (note that in this case, for the intermediate regime, α_n does appear to saturate for large n). The stronger nature of the flow causes the first stage to be very short, the intermediate stage is also relatively shorter as the filaments fill the domain quickly. Finally, the eigenmode is realized and persists till all the variance is destroyed.

In essence the picture that emerges is fairly straightforward, as long as there is a valid scale separation (i.e., till $l_s \ll l_v \sim L$), the pdf's of the scalar field are evolving entities, albeit involving stages characterized by a distinct decay of moments. Whereas, as soon as $l_s \sim l_v \sim L$, the scalar field enters an eigenmode with stationary or self-similar pdf's. Interestingly, some of our preliminary numerical work indicates that when we consider $l_v \ll l_s \sim L$, the self-similarity is maintained whereas the shape of the pdf is altered. In fact, smaller the scale of the velocity field the more Gaussian is the self-similar scalar pdf. As future work we plan to look deeper into these cases, especially in light of the recent results on nondiffusive asymptotic self-similarity of turbulent decay (i.e., where the advecting flows themselves are self-similar and nonsmooth), as put forth by Chaves *et al.* [34].

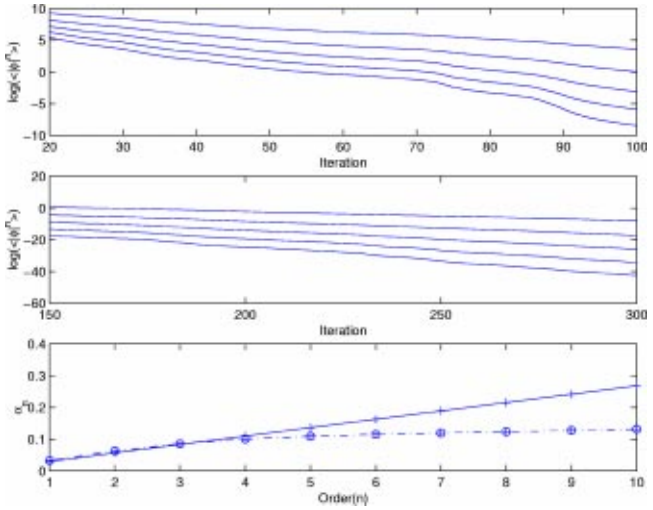

FIG. 11. Case with $A=C=5$ in Eq. (21). Upper two panels show the moments ($n=2$, 4, 6, 8, and 10 with higher moments appearing lower on the figure) and the lower panel shows α_n vs n extracted from iterations 20–70 (dashed line) and iterations 150–300 (solid line), respectively. Note the saturation of α_n in the intermediate regime. Log refers to the natural logarithm.

ACKNOWLEDGMENTS

We are indebted to Professor Peter Haynes for many valuable discussions and for providing access to an early version of the work by Feredey *et al.* [16], which led us to think of the line of research reported above. This work was supported by the National Science Foundation, under Grant Nos. ATM-9505190 and ATM-0123999.

[1] G. Batchelor, J. Fluid Mech. **5**, 113 (1959).
[2] J. Ottino, *The Kinematics of Mixing: Stretching, Chaos, and Transport* (Cambridge University Press, Cambridge, London, 1989).
[3] G. Falkovich, K. Gawedzki, and M. Vergassola, Rev. Mod. Phys. **73**, 913 (2001).
[4] R. Pierrehumbert and H. Yang, J. Atmos. Sci. **50**, 2462 (1993).
[5] Y. Hu and R. Pierrehumbert, J. Atmos. Sci. **58**, 1493 (2001).
[6] M. Chertkov, G. Falkovich, I. Kolokolov, and V. Lebedev, Int. J. Mod. Phys. B **10**, 2273 (1996).
[7] E. Balkovsky and A. Fouxon, Phys. Rev. E **60**, 4164 (1999).
[8] M. Jullien, P. Castiglione, and P. Tabeling, Phys. Rev. Lett. **85**, 3636 (2000).
[9] A. Majda and P. Kramer, Phys. Rep. **314**, 237 (1999).
[10] R. Pierrehumbert, Chaos, Solitons Fractals **4**, 1091 (1994).
[11] R. Pierrehumbert, Chaos **10**, 61 (2000).
[12] D. Rothstein, E. Henry, and J. Gollub, Nature (London) **401**, 770 (1999).
[13] T. Antonsen, Jr., Z. Fan, E. Ott, and E. Garcia-Lopez, Phys. Fluids **8**, 3094 (1996).
[14] A. Wonhas and J. C. Vassilicos, *Mixing in Fully Chaotic Flows* (Elsevier, in press).
[15] K. Gawedzki and M. Vergassola, Physica D **138**, 63 (2000).
[16] D. Fereday, P.H. Haynes, A. Wonhas, and J.C. Vassilicos, Phys. Rev. E **65**, 035301(R) (2002).
[17] B. Bayly, Phys. Rev. Lett. **57**, 2800 (1986).
[18] B. Bayly, Geophys. Astrophys. Fluid Dyn. **73**, 61 (1993).
[19] A. Soward, Physica D **76**, 181 (1994).
[20] T. Kato, *Perturbation Theory of Linear Operators*, 2nd ed. (Springer-Verlag, Berlin, 1980).
[21] S. Childress and A. Gilbert, *Stretch, Twist, and Fold: The Fast Dynamo* (Springer-Verlag, Berlin, 1995), Chap. 9.
[22] H. Aref, Phys. Fluids A **3**, 1009 (1991).
[23] B. Lingevitch and A. Bernoff, J. Fluid Mech. **270**, 219 (1994).
[24] J. Finn and E. Ott, Phys. Fluids B **2**, 916 (1990).
[25] V. Arnol'd, Y. Zel'dovich, A. Ruzmaikin, and D. Sokolov, Zh. Eksp. Teor. Fiz. **81**, 2052 (1981) [Sov. Phys. JETP **54**, 1083 (1981)].
[26] A. Crisanti *et al.*, *Products of Random Matrices in Statistical Physics* (Springer-Verlag, Berlin, 1993).

[27] J. Eckmann and I. Procaccia, Phys. Rev. A **34**, 659 (1986).
[28] P. Grassberger, R. Badii, and A. Politi, J. Stat. Phys. **51**, 135 (1988).
[29] E. Ott, *Chaos in Dynamical Systems* (Cambridge University Press, Cambridge, London, 1993).
[30] U. Frisch, *Turbulence* (Cambridge University Press, Cambridge, London, 1995).
[31] Y. Zel'dovich, A. Ruzmaikin, S. Molchanov, and D. Sokoloff, J. Fluid Mech. **144**, 1 (1984).
[32] T. Elperin, N. Kleeorin, and I. Rogachevskii, Phys. Rev. E **63**, 046305 (2001).
[33] W. Young, P. Rhines, and C. Garrett, J. Phys. Oceanogr. **12**, 515 (1982).
[34] M. Chaves, G. Eyink, U. Frisch, and M. Vergassola, Phys. Rev. Lett. **86**, 2305 (2001).